Available online at www.sciencedirect.com
SCIENCE DIRECT®
Journal of Power Sources 144 (2005) 244–254
JOURNAL OF POWER SOURCES
www.elsevier.com/locate/jpowsour

The influence of fast charging on the performance of VRLA batteries

V. Svoboda *, H. Doering, J. Garche

Center for Solar Energy and Hydrogen Research, Helmholtzstrasse 8, 89081 Ulm, Germany

Received 14 June 2004; received in revised form 3 December 2004; accepted 10 December 2004
Available online 11 February 2005

Abstract

A valve regulated battery (VRLA) with thin tubular electrodes combines the endurance of robust positive tubular electrodes and the enhanced power properties of very thin electrodes. Fast charging is essential for many applications and it can compensate the lower energy density of lead-acid batteries. Thin tubular electrodes VRLA batteries were cycle life tested and influences of two charging regimes were investigated. A comparison is made between a newly developed fast charging regime with current step-down and a conventional charging regime as regards battery life and performance. The fast charging procedure was beneficial for the cycle life; however, associated beneficial effects were reduced by certain drawbacks. A measuring method was developed for analysing the current distribution over the electrodes at high and low currents and results are presented in this paper. Post-mortem battery analyses were carried out to determine the dominating degradation effects. The differences in the degradation effects caused by the charging regimes are discussed. The paper concentrates on the newly developed fast charging regime and compares the influence of the charging regime on ageing mechanisms of the VRLA batteries with tubular electrodes as opposed to a conventional charging regime.

Keywords: Valve regulated lead-acid battery (VRLA); Thin tubular plates; Fast charging; Cycle life; Current distribution; Ageing

1. Introduction

An effort to reduce environmental pollution particularly in large urban areas and to reduce vehicles' fuel consumption requires changes in transportations. Electric vehicles (EV), hybrid electric vehicles (HEV) and internal combustion engine vehicles with additional features like start–stop function may be the optimal way to achieve such efforts. EVs and HEVs have some technical, financial and psychological drawbacks that prevent their success in the present market. Battery parameters, investment costs and charging represent some of the key problems.

Lead-acid batteries are cheap and on the other hand, they have limited energy density in comparison with other advanced energy storage technologies. In some applications (e.g. utility vehicles, fork-lift tracks) this drawback of lead-acid batteries may be overcome by fast charge. A fast battery recharge during short breaks in a utility vehicle operation results in nearly equal performance to vehicles with advanced batteries.

These assumptions initiated the development of lead-acid batteries with advanced performance and good fast charging capability together with the development of a fast charge with respect to the battery lifetime. The results of this research are of importance and may influence the penetration of the present market by EVs, HEVs and other battery applications where fast charging and high power performance is required. The results identify particular ageing mechanisms in lead-acid batteries at high rate operation that should be considered for further development of batteries.

1.1. How to control fast charging?

The main requirement for fast charging is minimal charging time without abuse to the battery. A fast charge that continuously adapts to the actual charge acceptance seems to be a promising method that respects the charging time and

* Corresponding author. Tel.: +49 731 9530602; fax: +49 731 9530666.
E-mail address: vojtech.svoboda@v-sv.com (V. Svoboda).

0378-7753/$ – see front matter © 2005 Elsevier B.V. All rights reserved.
doi:10.1016/j.jpowsour.2004.12.026

the battery lifetime. As the voltage is the central parameter for controlling the charge process it would be preferable to know the corresponding effective voltage (responsible for the charge transfer reaction) and to separate and if possible to compensate voltage fractions which only cover up the voltage of interest. The differences in the time constant of the voltage fractions can be used for the separation, e.g. during the voltage relaxation after current interruption.

Inductance of lead-acid batteries usually varies in the range of 10–100 nH Schleuter [4] and thus the inductance influence on the voltage curve is usually almost neglectable. The overpotential caused by the ohmic resistance has the time constant in the range of 10^{-7} s and the resistance can be measured. Therefore, the compensation of the ohmic resistance is the most popular technique for fast charge.

Compensation of other voltage losses such as diffusion overpotential would be beneficial; however, this requires several tens of seconds after the current interruption for online determination (Doering and Svoboda [3]) and is impractical for fast charging.

1.2. Fast charging by resistance-free charge voltage

The charge voltage (U_{ch}) is usually used to control the charge process and may be simplified by the equation:

$$U_{ch} = U^{o} + IR + \eta$$

However, from these parameters (U^{o}: open circuit voltage; IR: internal resistance part; η: polarisation) only the polarisation is directly linked to the electrode processes. Therefore, the charge voltage reduced by the internal resistance part (IR), the so-called resistance-free charge voltage (U^{*}_{ch}), is a better charge control parameter. It is expressed by the equation:

$$U^{*}_{ch} = U_{ch} - IR = U^{o} + \eta$$

The internal ohmic resistance compensation is very beneficial particularly at high charging current as it provides much more effective means of controlling charging. Kordesch [1] has originally introduced and published this principle already, early as in 1960 and used it for a charge control in 1972 [2]. By pulse-like interruption of the battery charging current, the voltage step-drop can be measured and the internal resistance can be calculated. A patent for resistance-free charge control was applied for by F.H. Mullersman in US Patent no. 3,531,706 in 1970, R.F. Chase in US Patent no. 3,576,487 in 1971 and later in many other patents.

Successful commercial fast chargers called MinitCharger (TM) providing *IR* compensation were manufactured by J. Nor at Norvik. Subsequent theories and discussions have shown that a fast charge using *IR* compensation techniques can prolong the cycle life of a battery due to various effects which reduce ageing, some of which are still being discussed.

1.3. Fast charging by pulse charge

If the current will be switched on, the potential will increase related to the same voltage fractions as at the current interruption with nearly the same time constants. Just before the charge potential reaching the gassing voltage, the current will be switched off. By a pulse-like repeating of switching on and off, one can avoid the gassing.

Pulse charge as a potential method for fast charge was also investigated at ZSW as part of the ALABC research project (Doering and Svoboda [3]). The results can be briefly summarised: in comparison with an equivalent constant current charge, a pulse charge would preferably require an individual electrode potential control (practically almost impossible), leads to higher Joule losses at the same average current and to longer charging time at the same maximal current rate. No influence on diffusion was observed. However, at the same time lower gassing and higher negative electrode polarisation at the end of charging was measured. Thus, the pulse charge has limited benefits. From our point of view pulse charge techniques seems to be not favourable with respect to fast charge.

2. New fast charge method—voltage controlled current step-down

In order to avoid the situation that the charge current is higher as the charge acceptance a charge technique requires a convenient charge control mechanism that keeps the charge process always close to the battery maximal charge acceptance. An important step to this control mechanism is the knowledge of the maximal charge acceptance as function of the state-of-charge (SOC) of the battery.

We have measured parameters of the tested valve regulated (VRLA) battery for different charging conditions in the current range of 0.2–3 C and in the SOC range of 0–100%. From the measured values we have constructed the *U*–*I*–SOC map depicted in Fig. 1. The pale curve in the map represents the border line between the area of dominating active mass charge and the overcharge area where the side reactions, particularly gassing are dominant. The use of higher charging rates/higher voltages over the border line leads to very excessive gas evolution, battery heating and other side effects. The graph demonstrates that, when using a sophisticated charge control mechanism, which prevents crossing the border line by reduction of the charge current, and voltage limit criteria with increasing SOC then very high charge current may be used.

The *U*–*I*–SOC map (Fig. 1) was the basic for our new developed fast charge regime.

The internal resistance is compensated in that way that the measured battery internal resistance behaviour was taken into consideration for the voltage limits of the individual current steps.

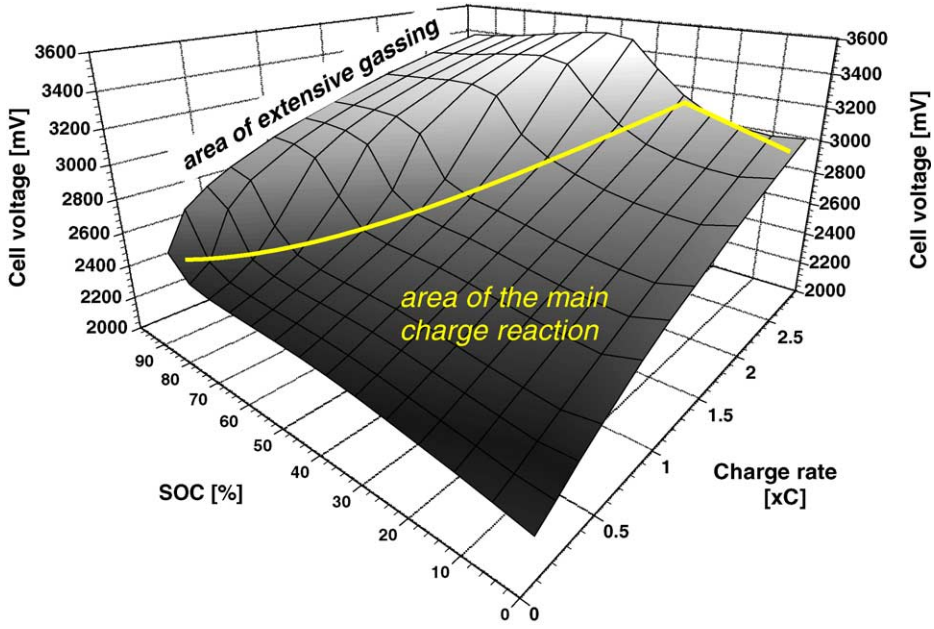

Fig. 1. *U–I*–SOC map measured on a VRLA battery.

The mentioned diffusion overpotential is empirically compensated.

Temperature compensated charging voltage limits ($-4\,\mathrm{mV\,K^{-1}}$ cell) provide effective control mechanism against temperature abuse.

The charge regime was finally tuned, considering minimal charge duration, minimal gassing and minimal temperature rise and thus the values were optimised to achieve the desired optimal charge performance throughout the entire cycle life.

So the developed, tested and optimised a new current step-down fast charging procedure is characterised by the high charge current steps just below the border line of the maximum charge acceptance, each current step controlled by well-defined respective voltage limits (see Fig. 2). Once in a certain current step the battery gets too close to the border line of maximum charge acceptance, automatically the charge step get terminated by the corresponding voltage limit causing the switching over to the next smaller charge current step. The number of the various individual current steps was chosen to be in a reasonable range. This charging method is very effective and universally adaptable for fast charging of almost every lead-acid battery.

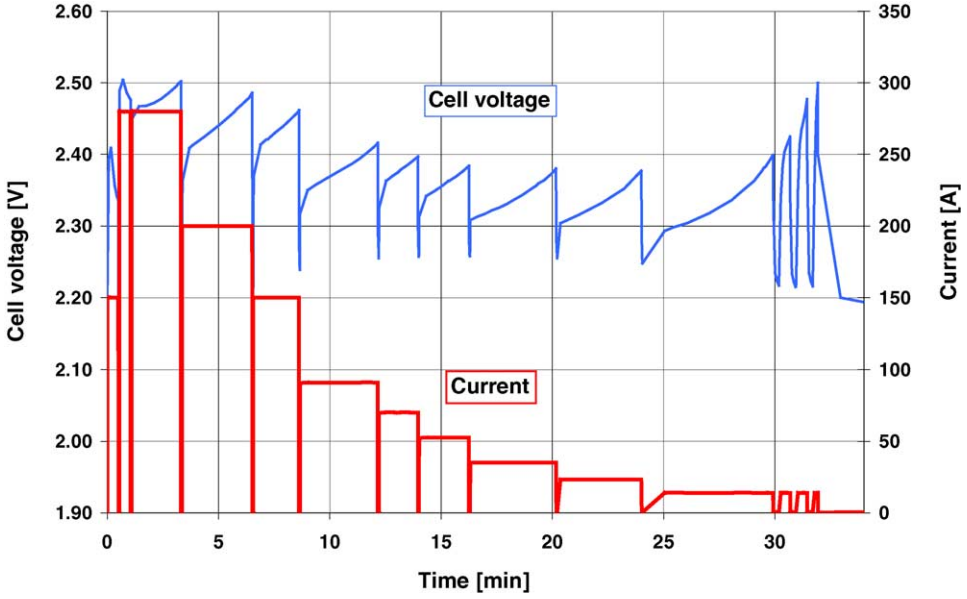

Fig. 2. Current step-down fast charging procedure.

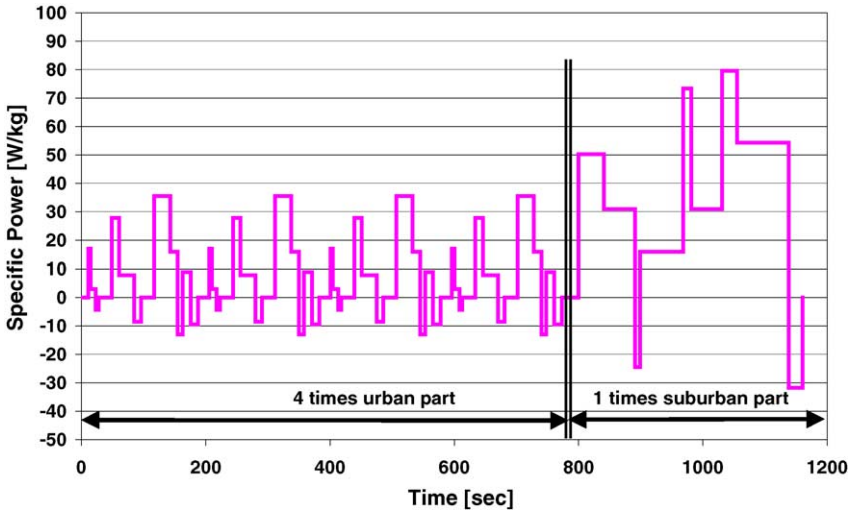

Fig. 3. Specific power profile of ECE15 dynamic discharge procedure, refer to [5].

Recharging of the last few percents of SOC requires very low charge current and thus long charging time. Practically fast charging cannot recharge batteries to 100% SOC due to the short charging time which is required.

The current step-down fast charge procedure is set to recharge the battery to approximately 95% SOC. Therefore, a regular full recharge is necessary to prevent undercharge degradation and to equalise the SOC of individual cells.

A particular problem is the negative electrode undercharge during fast charging. The results of the mentioned pulse charge research were applied and current pulses were introduced at the end of fast charging. Using a reference electrode, it was proven that the relatively low rate and long time current pulses (0.2 C for 30 s followed by 15 s rest time) at the end of charge increased the negative electrode polarisation while the positive remained unchanged and gassing remained at a minimum level. Thus, the risk of the negative electrode undercharging was reduced. Tests performed on the batteries proved that a short charging time was possible. The tubular plate VRLA batteries could be recharged to 80% SOC in about 30 min, recharge to 95% took approximately 60 min.

3. Experimental

The advanced lead-acid batteries suitable for EVs and HEVs were tested under the new current step-down fast charging regime as opposed to a conventional I–U–I_o–I_a charging regime.[1] Battery performance tests including laboratory cycle life tests were carried out and the results were evaluated. It was essential to examine the battery behaviour at high and low rate charging and to analyse the dominant ageing mechanisms causing a difference in the performance and in the cycle life.

[1] CC–CV–CC_o–CC_a.

3.1. Thin tubular VRLA battery

A battery suitable for fast charging requires high charge acceptance, and low internal resistance for minimal Joule losses. In relation to the power performance and the internal resistance, flat grid plates and spirally wound batteries are the most favourable. The typical positive tubular electrodes have enhanced mechanical endurance suitable for application in EVs and HEVs; however, the disadvantage is low power performance and low charge acceptance. The thin tubular valve regulated lead-acid batteries were designed to combine both advanced power performance and high mechanical endurance. The batteries were developed and produced by CMP Batteries Ltd.

The advanced VRLA batteries of the following parameters were used in all the described experiments: 70 Ah, 12 V block with adsorptive glass mat (AGM) separator, consisting of six positive 3.5 mm thick tubular electrodes and seven negative grid plates. Lead tin calcium alloy (Sn 1.2%, Ca 0.08%) was used for the thin cast spine current collectors for enhanced corrosion resistance. Spines of an elliptical cross-section (2.24 mm × 1.20 mm) were used for larger collector/positive active mass (PAM) interface area.

3.2. Cycle life tests

Two types of cycle life tests were carried out, capacity demand cycling at $C/2$ constant current discharging and power demand cycling at ECE15 (80% DOD) dynamic discharging, refer to Fig. 3 and the EUCAR specification [5]. The dynamic discharge has incorporated recharging pulses that simulate recuperative breaking.

The capacity demand cycling was performed in a room temperature; the power demand cycling was carried out in a controlled water bath at 35 °C. The end of battery lifetime was set at 60% of the initially measured capacity at the corresponding discharge profile.

Life cycle tests were carried out on five 12 V blocks connected in series.

Fast current step-down and conventional I–U–I_o–I_a charging was used in both types of cycling. The conventional I–U–I_o–I_a charging regime was used as reference experiments. The conventional charge maximum inrush current rate was limited to $C/5$; the constant voltage charging phase was terminated when the current fell below $C/28$. Two final constant current charging phases were carried out at a current rate of $C/35$ and $C/70$. These steps were limited both as regards voltage and time. The parameters of the conventional charging regime were specified by the battery manufacturer. A typical time duration of the conventional charging regime is 6–12 h.

The current step-down fast charging regime was used in the experiments in this sequence: four fast charging cycles followed by one conventional charging cycle. This cycling simulates an EV utility vehicle operation; the fast recharge is performed during the day-time and the full conventional charge overnight.

3.3. Current distribution over the electrode

A homogeneous current distribution over the electrode's plate is beneficial for uniform active mass utilisation. Current distribution over the electrodes was evaluated at high and low charge and discharge current. A method for measuring and analysing was proposed and implemented for this purpose.

In principle, the method is based on a voltage measurement on a variable shunt while the shunt is regularly calibrated. The negative electrode's plate represents the variable resistance shunt. The resistance of the negative electrode's plate that varies at charging and discharging is "calibrated" by regular, constant current injections (current pulses of 1 A for 5 s from an external power source). The current pulses are injected geometrically symmetrical on the electrode's plate surface. The current injections are applied to the negative electrode plate during regular interruptions of the battery current. A measurement of the voltage distribution on the electrode's plate surface during the current injections makes it possible to create an actual potential map. In that time the actual potential map is equal to the situation of the homogeneous current distribution on the electrode's plate because the actual potential map is invoked by symmetrically distributed same current pulses.

The final results are achieved by comparing the actual potential maps with time corresponding measured potential maps during charging, respectively, discharging of the battery. The method can be applied with sufficient precision to measure and analyse the current distribution in the electrode.

3.4. Evaluation of ageing mechanisms

Evaluation of the intensity of individual ageing mechanisms was done within post-mortem analyses after end of the battery cycling. Besides chemical analyses of the positive and negative active mass in order to indicate hard/irreversible sulphation, also other analyses techniques were applied to indicate the dominating ageing mechanisms.

AM particle size analysis was carried out by means of Malvern Instrument Flow Particle Image Analyzer FPIA-2100FPIA and proved by scanning electron microscope (SEM). The FPIA method uses fast CCD camera photography of particles in the sample. Negative active mass (NAM) samples were only analysed using the SEM method.

The porosity of positive active mass also measured by a mercury porosimetry technique. We used for the analysis Porosimeter 2000 produced by Carlo Erba Instrument Co.

The positive electrode corrosion was evaluated by light microscope examination of the tubes' cross-section. The tubes gauntlets and PAM were mechanically removed and the spines current collector system was chemically cleaned by alkaline-sugar solution to remove lead-oxide (Garche [6]). Then the spines surface was again examined by light microscope.

4. Results and discussion

4.1. Cycle life results

Results of cycle life measurements are summarised in Table 1.

The capacity demand cycling was stopped at the same capacity level of approximately 60% of the rated capacity. The difference in the cycle life results indicated an approximately 40% longer cycle life for batteries with fast charging.

For the power demand cycling every 50th cycle regular capacity check-ups consisting of conventional charge and constant current $C/5$ discharge were done on both the conventional and the fast charged battery.

The power demand cycling was stopped when the ECE15 capacity dropped below 60% (39 Ah) of initially measured ECE15 capacity (65 Ah).

Table 1
Cycle life results at fast and conventional charge

Test	Charge regime	Cycling regime	No. of cycles	$C/5$ capacity (Ah)	ECE15 capacity (Ah)
Capacity demand	Conventional	$C/2$	670	40	–
	Fast	$C/2$	930	40	–
Power demand	Conventional	ECE15	436	50	37.0
	Fast	ECE15	469	62	37.1

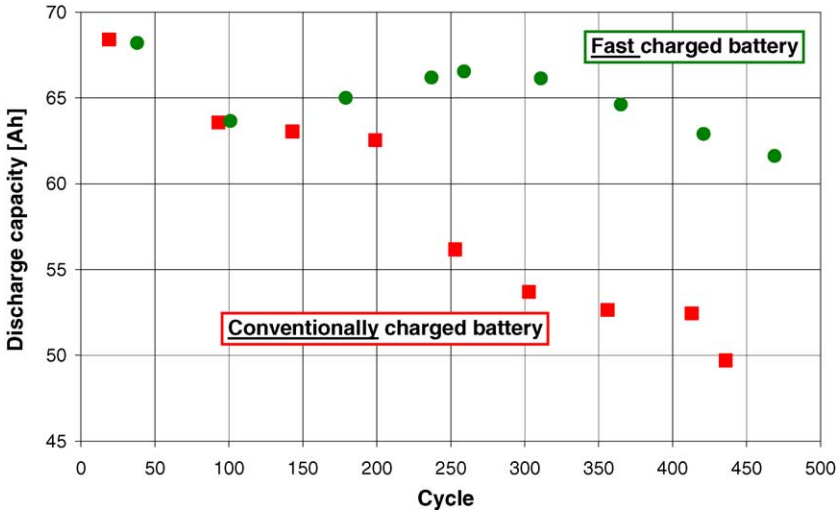

Fig. 4. *C*/5 capacity measured during the regular capacity check-ups carried out each 50 cycles of the ECE15 profile for conventional and fast charged batteries.

The difference in discharge performance under the dynamic discharge conditions of the ECE15 was minimal. However, comparing the batteries in the *C*/5 discharge capacity tests (see Fig. 4) a significant higher capacity was measured for the fast charged battery. The loss of power performance was similar under both charge regimes but fast charge reduced the loss of *C*/5 capacity significantly.

4.2. AM utilization

Each cell of the battery contains 1080 g of the positive active mass and 1015 g of the negative active mass. The theoretical capacity corresponding to the PAM and NAM amount is 242 and 263 Ah, respectively.

The PAM and NAM utilisation in relation to the initial *C*/5 discharge capacity (70 Ah) is 29 and 27%, respectively. The PAM and NAM utilisation in relation to the initially measured ECE15 capacity (65 Ah) is 27 and 25%, respectively.

4.3. Current distribution analysis

The proposed method for measuring the current distribution on the negative electrodes was successfully realised. The results for these measurements are shown in Fig. 5 for a charge current of 0.3 and 1.6 C and 30% charge return and Fig. 6 for 0.2 C charge and 105% charge return.

A summary of the current distributions which were analysed shows:

- Higher currents lead to a less homogeneous current distribution and a lower relative current density at the bottom of the electrodes. The surface charts in Fig. 5 represent the measured deviation from the homogeneous current distribution under 0.3 and 1.6 C charge rate.
- It was found that the effect of current rate influence on the current distribution is stronger at charging in comparison with discharging.
- Complete recharging of the bottom of the electrodes is achieved only if close to 100% SOC. The surface chart in

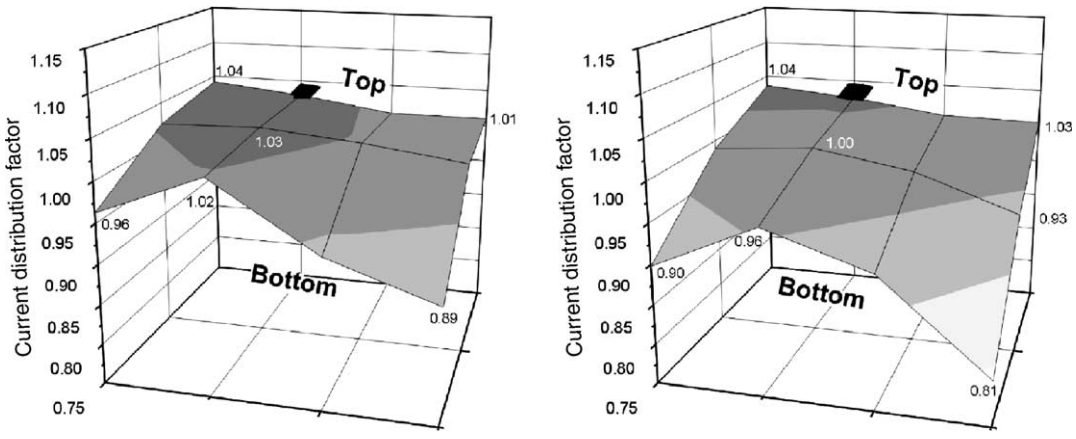

Fig. 5. Surface charts of the negative plate representing deviation from homogeneous current distribution over the electrode plate. Left: charge rate 0.3 C; right: charge rate 1.6 C; 30% charge return. The black square represents the plate lug at the top of the plate.

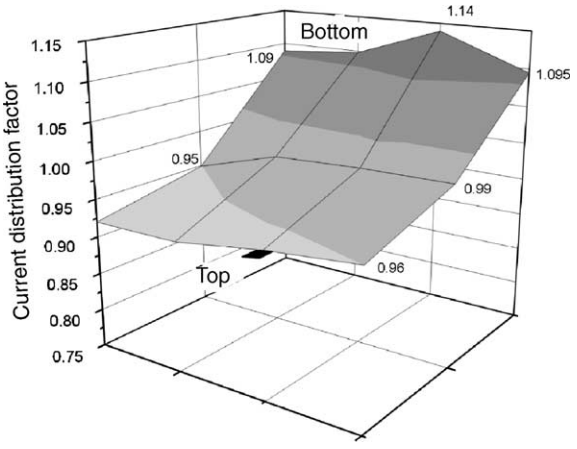

Fig. 6. Surface chart of the negative electrode representing deviation from homogeneous current distribution over the electrode plate. Charge rate 0.2 C, 105% charge return. The black square represents the plate lug at the top of the plate.

Fig. 6 represents the recharge of the electrode bottom part; such current distribution was measured at 105% charge return.

The results may be explained by the electrode plates' resistance together with the dependence curve of the current on the charge-transfer over-potential which is expressed by the Butler–Volmer equation. The measured current distributions are consistent with simulation results published by Calabek [7].

4.3.1. Limiting electrode

The battery is designed with an oversized negative electrode capacity in relation to the positive electrode. At the end of the cycle life the electrode which limits the discharge was identified by reference electrode measurements.

After the power demand ECE15 cycling the positive electrode was the limiting electrode in both cases independently of the charge regime. This correlates to the originally over sizing of the negative electrode which is still the case after relatively low number of cycles (about 450 ECE15 cycles).

For the capacity demand cycling at the end of cycle life the negative electrode was capacity limiting indicating that the performance loss of the negative electrode at the higher number of cycles (670 and 930 cycles for the conventional and fast charged battery, respectively) got in the range that the original over sizing is not effective any more.

The current step-down fast charging may better preserve the performance of the negative electrode and in this way may lead to a prolongation of cycle life. Unfortunately, the longer cycle life for the fast charged batteries was associated with a low power operation only (refer to Table 1).

4.3.2. Water loss—gassing

The total water loss at the end of the cycle life of conventionally charged battery of 67 g per cell was approximately 65% higher compared to the water loss of 40.5 g per cell of fast charged battery. Lower average gassing (average of the sequence: four fast charging cycles followed by one conventional charging cycle) at fast charged batteries compared to conventionally charged batteries was proven by measuring the amount of gas released from individual cycles during charging.

With fast charged batteries, lower gassing and lower total water loss and higher charge Coulombic efficiency and lower overall charge factor were measured in comparison with batteries which were conventionally charged. The lower gassing at fast charged batteries is due to the lower average charge factor, due to shorter duration of charge polarisation demonstrated later in this paper, due to the effective charge control and due to kinetic factors.

4.3.3. Hard/irreversible AM sulphation

Before being opened, the batteries were fully conventionally charged and then the AM samples were chemically analysed. Higher hard/irreversible sulphation was detected in the fast charged batteries particularly at the bottom of both electrodes. The results of the hard/irreversible lead sulphate content analysis at the end of the cycle life are summarised in Table 2. The fast charged batteries suffered more from hard/irreversible sulphation due to the higher charge current that is less homogeneously distributed in the electrodes and also due to undercharging as a result of frequent and regular recharging to less than 100% SOC (refer to Section 4.2). The undercharge is the result of the fast cycling sequence of four fast charging cycles and one conventional charging cycle. Fast charging recharges the battery to only approximately 95% SOC. In Section 4.2 it was also concluded that the bottom of the electrodes is only fully recharged if the SOC gets close to 100%.

4.3.4. Electrolyte stratification

A tendency to higher electrolyte stratification was measured in the fast charged batteries compared to the conventionally charged batteries. The analysed electrolyte gravity of the fast charged battery at the top part was 1.26 g cm^{-3}, while at the bottom part 1.31 g cm^{-3} and of the conventionally

Table 2
Results of the hard/irreversible lead sulphate content analysis at the end of life

Content of $PbSO_4$	Fast charged (%)		Conventionally charged (%)	
	Positive plate	Negative plate	Positive plate	Negative plate
Top part	14.1	9.9	9.6	11.1
Bottom part	19.4	32.9	6.3	11.2

charged battery at the top 1.28 g cm^{-3}, while at the bottom 1.31 g cm^{-3}. In the fast charged batteries, there is lower current density at the bottom and a higher current density at the top of the electrode. The higher charging current leads to the diffusion of higher density acid out of the top of the electrodes than out of the bottom. Thus, the gravitational force causes a downward flow of the acid with higher density. Although the electrolyte stratification is hindered in the VRLA batteries, due to relatively immobilised electrolyte in the AGM separator, there is still a downward drift of the higher density electrolyte in the gaps in between the electrodes and the separators and, equally, re-mixing of electrolyte is hindered, too.

The electrolyte stratification builds up higher density electrolyte at the bottom causing higher local electrochemical potential which at one hand, discharges the electrodes at the bottom and recharges at the top and on the other hand, it reduces the recharging of the electrodes at the bottom even more and leads directly to hard/irreversible sulphation.

4.3.5. Positive electrode current collector corrosion

The degree of corrosion of the spines of the positive electrode after cycling was observed by means of a light microscope. The cross-sections of the tubes of the positive electrodes (shape of remaining spines and the corrosion corona) and also the cleaned surface of spines are shown in Fig. 7. The pictures indicate that the degree of corrosion of the spines differs significantly. The fast charged batteries suffer less from positive electrode grid corrosion than the conventionally charged batteries.

This unexpected phenomenon can be explained by the dependence of lead corrosion on the polarisation in diluted sulphuric acid electrolyte, reported by Lander [8], and by the histograms of the potential in Fig. 8. There is higher specific lead corrosion at lower and at higher polarisation. As a result of fast charging, the grid quickly leaves the lower polarisation region and brings the electrode at first to the passivation region at higher polarisation. Later fast charging polarises the electrode to higher potentials which accelerates corrosion; however, the absolute time of high polarisation of the electrode is much shorter during fast charging than during conventional charge; see histogram in Fig. 8.

4.3.6. SEM pictures of PAM

After the cycling, samples of the positive active mass of the conventionally (436 cycles) and of the fast charged battery (469 cycles) were collected from the top electrode's parts. The samples were analysed by scanning electron microscope. It was observed that PAM particles of the fast charged battery were smaller in comparison to the PAM particles of the conventionally charged battery. It also seemed that the porosity of the sample of the fast charged battery is lower to the porosity of the sample of the conventionally charged battery. Fig. 9 shows SEM pictures of the PAM samples from the conventionally charged battery after 436 cycles and of the fast charged battery after469 cycles.

4.3.7. AM particle size

The results of the FPIA particle size measurements of the positive active mass samples from the top of the electrodes are listed in Table 3.

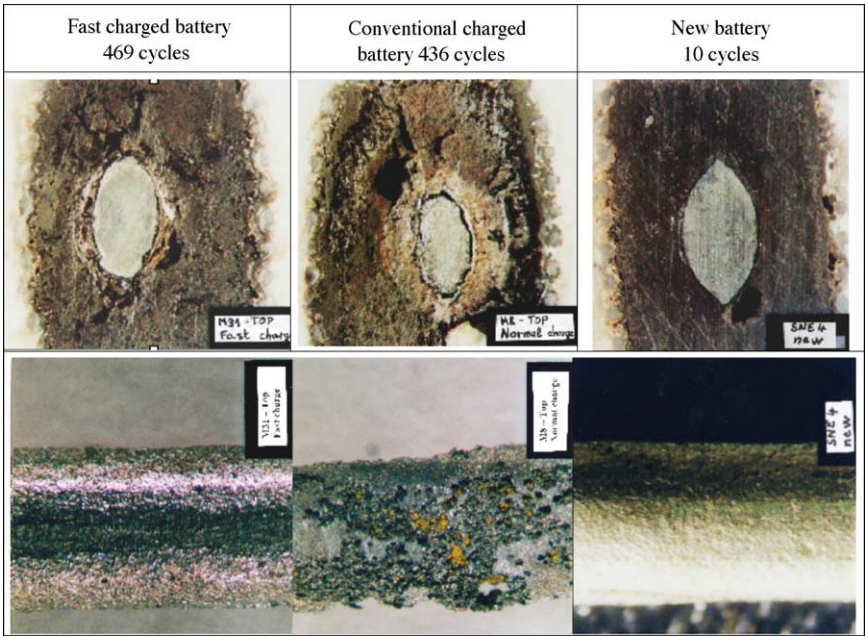

Fig. 7. Light microscope photos of the positive electrodes' cross-sections (top row) and the spines' surfaces (bottom row).

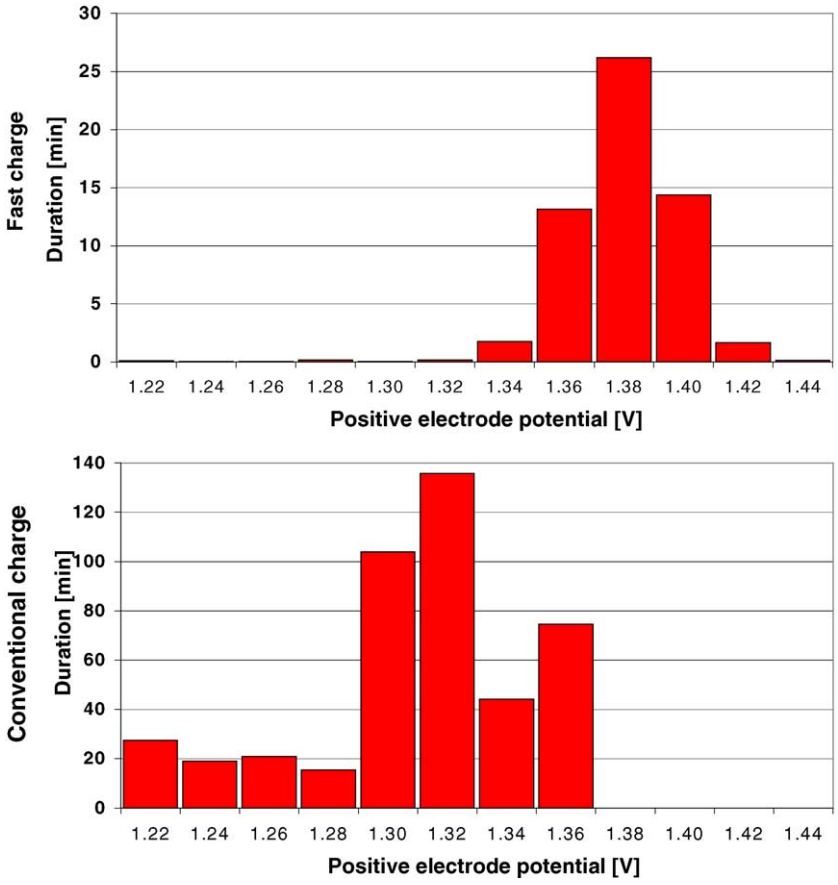

Fig. 8. Positive electrode potential histogram at fast (top) and conventional charge (bottom); measured vs. Hg/Hg_2SO_4 reference electrode.

This is in agreement with the expectations that high charging currents support the generation and growth of smaller crystals. The particle size measurement on the PAM samples from the fast charged batteries, electrode bottom part, indicated much more larger particles due to the reported high sulphation of the bottom electrode parts.

The PAM agglomerates of the conventionally charged batteries appeared to be less stiff and less compact than the PAM agglomerates from the fast charged batteries. It was indicated by the PAM agglomerates stability during an ultrasonic mixing in water medium.

In summary it can be concluded that fast charged batteries have a tendency to maintain the initial stiff small AM particle size structure.

4.3.8. AM porosity

Results of PAM porosity measured by the mercury porosimetry method are summarised in Table 4.

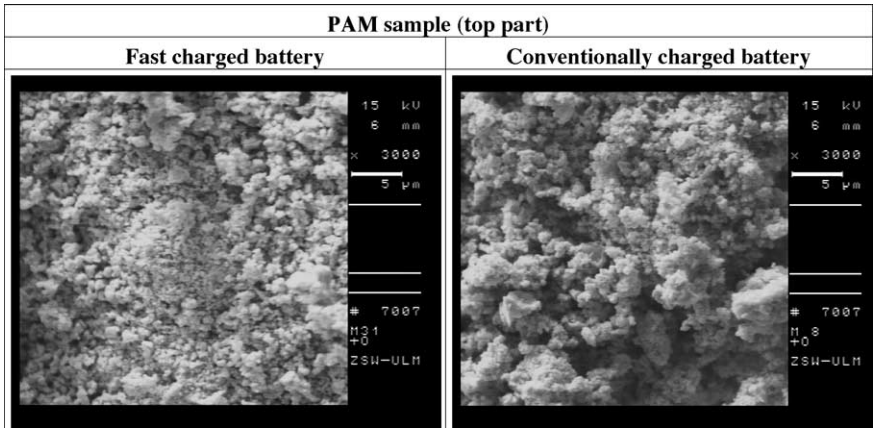

Fig. 9. SEM pictures of PAM samples. Left: fast charge battery, 436 cycles; right: conventionally charged battery, 469 cycles.

Table 3
Results of FPIA particle size analysis at end of the cycle life

PAM sample	Mean particles diameter (μm)	
	Fast charged battery	Conventional charged battery
Top part	2.21	2.79

Table 4
Average PAM porosity at the fast cycled battery after 469 cycles, at the conventionally cycled battery after 436 cycles, and the new cell

	PAM porosity (%)
Fast charged battery	53.4
Conventionally charged battery	58.9
New cell	52.8

The average results of the top–bottom samples indicate that the PAM porosity tends to rise at cycling. The fast charging process leads to a moderate porosity increase in comparison with conventional charging. The porosity increase may be explained by the PAM expansion. The aged PAM structure is less stiff with smaller conductive necks between the particles; the process is described by so called Kugelhaufen model (Winsel [9]). Furthermore, the PAM expansion is forced by sulphation.

4.4. Summary of different degradation effects

Different degradation effects were found to dominate in conventionally and fast charged batteries. In conventionally charged batteries, the dominating degradation effects seem to be the corrosion of the positive electrode current collector which leads to degradation changes of the PAM-current collector interface, the degradation of the structural properties of the bulk PAM and the drying out process.

The dominating degradation effects in fast charged batteries are hard/irreversible sulphation, the less homogeneous current distribution that leads to undercharging and severe degradation at the bottom of the electrodes and the tendency to higher electrolyte stratification.

5. Summary

The results discussed in the paper indicate that lead-acid batteries should be considered for use in advanced applications today and also in the future. The relatively low energy density which limit their use may be compensated for by a fast recharge and thus battery utilisation, e.g. in an EV may rise significantly. The research results may be applied in EVs, HEVs, for power load levelling in stationary systems and also in renewable energy systems.

The newly developed current step-down fast charging regime was optimised for VRLA batteries with thin tubular electrodes. The VRLA batteries can be recharged to 80% SOC in less than 30 min. The total water loss caused by gassing is reduced by 65% in comparison to conventional charging and thus reducing the drying out risk significantly. The charging regime has features which allow adaptation to almost every battery type and optimisation of the desired charging regime. Fast charging does not harm the battery and it was proved to be an excellent and reliable charging regime for VRLA batteries.

Fast charging usually recharges the battery to approximately 95% SOC. A regular full charge is very important in order to prevent undercharge degradation, and to equalise the SOC of individual cells. Although a full recharge of the fast charged battery was carried out, regularly at every fifth cycle, hard/irreversible sulphation was higher than in conventionally charged batteries particularly at the bottom of the electrodes.

Results of the measured and analysed current distribution during fast charging indicated the drawbacks which prevent much longer cycle life prolongation. Using this method, less homogeneous current distribution was measured for higher currents and poor recharge at the bottom of the electrode was detected as a particular problem. A design modification for batteries for fast charging should be considered to improve the current distribution. Such design modifications may affect the connection of the electrodes such as alternating top–bottom connection or both sides to be connected, etc.

The negative electrode becomes capacity determining at higher cycle numbers. The better condition of the negative electrode as a result of fast charging is a possible explanation for the significant prolongation of cycle life. The better condition of the negative electrode is the result of smaller particles and the high porosity which is preserved. Thus, fast charging prevents leading of the NAM. The AM structure of the positive electrodes in a fast charged battery was also protected. The PAM of the fast charged battery was more compact and stiff. Fast charging prevents softening of PAM.

Furthermore, it was found that fast charging led to significant corrosion protection of the positive electrode current collector.

The tendency to higher electrolyte stratification measured in the fast charged batteries together with higher sulphation on the bottom of the electrodes limit the performance of the fast charged battery at a high power discharge.

The dominating degradation effects of fast charging are hard/irreversible sulphation, electrolyte stratification and the less homogeneous current distribution that causes the severe degradation at the bottom of the electrodes. During conventional charging, the dominating degradation effect is the corrosion of the positive electrode current collector together with PAM softening, NAM leading and drying out.

Acknowledgments

This work was financially supported by the European Community under the Brite/Euram program BRPR-CT97-0602 and by the ALABC–ILZRO.

References

[1] K.V. Kordesch, Sine wave current tester for batteries, J. Electrochem. Soc. 107 (6) (1960) 480–483.
[2] K.V. Kordesch, Charging method for batteries, using the resistance free voltage as endpoint indication, J. Electrochem. Soc. 119 (8) (1972) 1053–1055.
[3] H. Doering, V. Svoboda, Influence of pulse charge currents on the specific energy, life and charging time of advanced tubular design, in: 6th ALABC Members & Contractors Conference, May 2–4, Kissimmee, FL, USA, 2001.
[4] W. Schleuter, Ein Beitrag zur Beschreibung des Elektrischen Verhaltens von Blei-, Nickel-Cadmium und Nickel-Eisen-Akkumulatoren, Ph.D. Thesis, Rheinisch-Westfaelischen Technischen Hochschule Aachen, November 1982.
[5] Specification of Test Procedures for Electric Vehicle Transportation Batteries, EUCAR Traction Battery Working Group, December 1996.
[6] J. Garche, Corrosion of lead and lead alloys: influence of the active mass and of the polarization conditions, J. Power Sources 53 (1995) 85–92.
[7] M. Calabek, Current distribution over the electrode surface in a lead-acid cell during discharge, J. Power Sources 105 (1) (2002) 35–44.
[8] J. Lander, Further studies on the anodic corrosion of lead in H_2SO_4 solution, J. Electrochem. Soc. 103 (1956) 1–8.
[9] A. Winsel, The aggregate-of-spheres (Kugelhaufen') model of the PbO_2/PbO_4 electrode, J. Power Sources 30 (1990) 209.